

See discussions, stats, and author profiles for this publication at: <https://www.researchgate.net/publication/41577068>

Sequential Adsorption of Bovine Mucin and Lactoperoxidase to Various Substrates Studied with Quartz Crystal Microbalance with Dissipation

ARTICLE *in* LANGMUIR · FEBRUARY 2010

Impact Factor: 4.46 · DOI: 10.1021/la902267c · Source: PubMed

CITATIONS

29

READS

15

4 AUTHORS, INCLUDING:



[Tobias J Halthur](#)

10 PUBLICATIONS 303 CITATIONS

SEE PROFILE



[Lubica Macakova](#)

YKI Institute for Surface Chemistry

14 PUBLICATIONS 364 CITATIONS

SEE PROFILE



[Adam Armitage Feiler](#)

KTH Royal Institute of Technology

25 PUBLICATIONS 903 CITATIONS

SEE PROFILE

Sequential Adsorption of Bovine Mucin and Lactoperoxidase to Various Substrates Studied with Quartz Crystal Microbalance with Dissipation

Tobias J. Halthur,^{*,†,§} Thomas Arnebrant,[†] Lubica Macakova,[‡] and Adam Feiler[‡]

[†]Biomedical Laboratory Science and Technology, Faculty of Health and Society, Malmö University, SE-205 06 Malmö, Sweden, and [‡]YKI, Institute for Surface Chemistry, Box 5607, SE-114 86 Stockholm, Sweden. [§]Present address: Colloidal Resource AB, Box 124, SE-221 00 Lund, Sweden.

Received June 24, 2009. Revised Manuscript Received February 12, 2010

Mucin and lactoperoxidase are both natively present in the human saliva. Mucin provides lubricating and antiadhesive function, while lactoperoxidase has antimicrobial activity. We propose that combined films of the two proteins can be used as a strategy for surface modification in biomedical applications such as implants or biosensors. In order to design and utilize mixed protein films, it is necessary to understand the variation in adsorption behavior of the proteins onto different surfaces and how it affects their interaction. The quartz crystal microbalance with dissipation (QCM-D) technique has been used to extract information of the adsorption properties of bovine mucin (BSM) and lactoperoxidase (LPO) to gold, silica, and hydrophobized silica surfaces. The information has further been used to retrieve information of the viscoelastic properties of the adsorbed film. The adsorption and compaction of BSM were found to vary depending on the nature of the underlying bare surface, adsorbing as a thick highly hydrated film with loops and tails extending out in the bulk on gold and as a thinner film with much lower adsorbed amount on silica; and on hydrophobic surfaces, BSM adsorbs as a flat and much more compact layer. On gold and silica, the highly hydrated BSM film is cross-linked and compacted by the addition of LPO, whereas the compaction is not as pronounced on the already more compact film formed on hydrophobic surfaces. The adsorption of LPO to bare surfaces also varied depending on the type of surface. The adsorption profile of BSM onto LPO-coated surfaces mimicked the adsorption to the underlying surface, implying little interaction between the LPO and BSM. The interaction between the protein layers was interpreted as a combination of electrostatic and hydrophobic interactions, which was in turn influenced by the interaction of the proteins with the different substrates.

Introduction

It is well-known that the mucosal membranes present in the respiratory tract and the gastrointestinal tract act as a protective barrier (being antiadhesive and yet acting as a selective mediator) between the external environment and the body. The outermost layer of these membranes is the highly hydrated (approximately 90% water content)^{1,2} viscous mucus in which the mucin proteins act as a scaffold. Although mucin by itself forms a viscous hydrogel, it is believed that the interaction of mucin with smaller proteins and salts affects the structure of mucin and gives mucus its exceptionally high viscosity,^{3,4} and also affects its lubricating effect in saliva.^{5,6}

Mucin is a diverse group of proteins that vary in size and composition depending on the source (human or animal) and type (membrane or secreted).² Mucin consists of large macromolecule monomers with a polypeptide backbone which contains one or more heavily glycosylated domains, rich in serine and threonine residues which serve as anchoring points for the oligosaccharide side chains. These glycosylated domains are separated by short “naked” nonglycosylated patches. The carbohydrate weight

fraction is substantial, and values between 68 and 81% have been reported.^{7,8} Because of the high concentration of oligosaccharides, the glycosylated domains are hydrophilic; they are also negatively charged due to the presence of sialic acid residues and sometimes also due to the presence of sulfated sugars. The “naked” patches and the end terminals (which are also nonglycosylated regions) on the other hand contain a normal distribution of amino acid residues and are mostly hydrophobic. Furthermore, cysteine residues are located in the end terminals, which provides for intra- and intermolecular disulfide bonds. According to a model for human cervical mucin first proposed by Carlstedt and Sheehan, several mucin monomers are linked together by disulfide bonds in a linear chain. This particular mucin carried four monomers on average, and each monomer contained four to five glycosylated domains.⁹

Lactoperoxidase is a cationic enzyme, with an isoelectric point of 8.3 and a net charge of +4 eq/molecule at pH 7.0, that catalyzes the oxidation of halides and pseudohalides by the aid of hydrogen peroxide, and generates highly reactive products with a wide antimicrobial activity.¹⁰ The polypeptide backbone consists of a single polypeptide chain of 612 amino acids with a molecular mass of 78.5 kDa and a carbohydrate content of about 10%. It also contains 14 cysteine residues, out of which 12 are involved in internal disulfide bridges and two are free sulfhydryl groups.¹¹ Lactoperoxidase has been found to be very stable and keeps its

*To whom correspondence should be addressed. E-mail: tobias@halthur.com.

(1) Matthes, I.; Nimmerfall, F.; Sucker, H. *Pharmazie* **1992**, *47*, 609–613.
(2) Strous, G. J.; Dekker, J. *Crit. Rev. Biochem. Mol. Biol.* **1992**, *27*, 57–92.
(3) Feiler, A. A.; Sahlholm, A.; Sandberg, T.; Caldwell, K. D. *J. Colloid Interface Sci.* **2007**, *315*, 475–481.
(4) Feldtö, Z.; Pettersson, T.; Dedinaite, A. *Langmuir* **2008**, *24*, 3348–3357.
(5) Hahn Berg, I. C.; Lindh, L.; Arnebrant, T. *Biofouling* **2004**, *20*, 65–70.
(6) Pettersson, T.; Dedinaite, A. *J. Colloid Interface Sci.* **2008**, *324*, 246–256.
(7) Loomis, R. E.; Prakobphol, A.; Levine, M. J.; Reddy, M. S.; Jones, P. C. *Arch. Biochem. Biophys.* **1987**, *258*, 452–464.
(8) Thomsson, K. A.; Prakobphol, A.; Leffer, H.; Reddy, M. S.; Levine, M. J.; Fisher, S. J.; Hansson, G. C. *Glycobiology* **2002**, *12*, 1–14.

(9) Carlstedt, I.; Lindgren, H.; Sheehan, K. *J. Biochem. J.* **1983**, *213*, 427–35.
(10) Kussendrager, K. D.; van Hooijdonk, A. C. *Br. J. Nutr.* **2000**, *84*(Suppl 1), S19–25.
(11) Boscolo, B.; Leal, S. S.; Ghibaldi, E. M.; Gomes, C. M. *Biochim. Biophys. Acta* **2007**, *1774*, 1164–1172.

enzymatic activity up to a temperature of 70 °C where it unfolds its hydrophobic core.¹¹

Mucin and lactoperoxidase are both natively present in the human saliva, and it has been shown that they can interact and form multilayers.¹² We believe that combining the antiadhesive barrier function of mucin with the antimicrobial activity of lactoperoxidase could be an interesting strategy for creating surface coatings for biomedical applications such as implants and sensors. However, in order to exploit the use of the complex biofilm, it is vital to gain information on the adsorption properties of the individual proteins and also on how the proteins interact with each other on different substrate surfaces. We have therefore used the quartz crystal microbalance with dissipation (QCM-D) technique to measure the adsorption properties of bovine mucin (BSM) and lactoperoxidase (LPO) on a variety of surfaces. In addition to adsorbed amounts and adsorption kinetics, the viscoelastic properties of the adsorbed films have been studied and compared.

Materials and Methods

Materials. Bovine submaxillary gland mucin (BSM) with a molecular weight of about 7×10^6 g/mol¹³ was purchased from Sigma (cat no. M-3895) and used as received.

Buffer salts sodium phosphate ($\text{Na}_2\text{HPO}_4 \cdot 12\text{H}_2\text{O}$) pro analysis grade and sodium phosphate ($\text{Na}_2\text{HPO}_4 \cdot 12\text{H}_2\text{O}$) were purchased from Merck. Solutions were prepared using ultrapure water (Milli-Q) (Milli-Q plus system, Millipore). Solutions and buffers were used fresh or stored overnight at 4 °C. The buffer solution used was a 10 mM phosphate buffer supplemented with 50 mM NaCl and adjusted to pH 7.0.

QCM-D measurements were performed on AT-cut 5 MHz quartz crystals, purchased from Q-Sense AB (Göteborg, Sweden). Three types of surfaces with different outer layers were used: Gold and hydrophilic silica surfaces were simply cleaned prior to use (see the experimental procedure), while the hydrophobic surfaces were created by treating hydrophilic silica-coated crystals following a simple protocol where they were first rinsed with Milli-Q and ethanol, gently dried with a stream of nitrogen gas, and then treated in a plasma cleaner (Harrick Scientific Corp., model PDC-32 G, Ossining, NY) in low-pressure air at 30 W for 5 min. The surfaces were then left overnight in a evacuated excicator together with a beaker containing a few milliliters of chloro-(dimethyl)octylsilane. The next day, the surfaces were rinsed and sonicated three times for 5 min in trichloroethylene and then three times in ethanol, and finally rinsed and stored in ethanol.

QCM-D. A QCM-D device is an instrument with the capacity of simultaneously measuring the resonant frequency shift (Δf) and the change in energy dissipation (ΔD). The theory of the instrument is described in detail by Rodahl et al.¹⁴ A thin piezoelectric AT-cut quartz crystal with metal electrodes deposited on each side is used as substrate surface. The quartz crystal can be excited to oscillate in shear mode at its resonant frequency f_0 (or at different overtones), by applying an AC voltage across the electrodes. Adsorption of a small mass (Δm) onto the crystal induces a decrease in the resonant frequency (Δf). Provided that the mass adsorbed is much smaller than the mass of the crystal, is evenly distributed, does not slip on the electrode surface and is sufficiently rigid and/or thin to have negligible internal friction, the frequency change Δf is directly proportional to the adsorbed mass Δm according the Sauerbrey equation.¹⁵

$$\Delta m = -\frac{\Delta f}{nC} \quad (1)$$

where C is the mass-sensitivity constant ($5.72 \text{ m}^2 \text{ Hz mg}^{-1}$ at $f_0 = 5 \text{ MHz}$) and n is the overtone number. The mass calculated from this relation is however the total mass oscillating with the crystal, that is, protein film plus coupled and trapped water. The Sauerbrey equation has been suggested to be a good approximation when the change in dissipation is less than 10^{-6} per 5 Hz of Δf .¹⁶ For dissipative, viscoelastic layers, such as those studied in the current work, the Voigt model is more appropriate and has been used here for analysis. We obtained good fits of our data using a commercial Q-tools program (Q-sense AB, Sweden), and we were able to resolve properties of the adsorbed layers in terms of their sensed mass, viscosity, and shear elasticity modulus. The adsorbed film was modeled as a uniform layer, and thus, resulting values correspond to average (effective) properties of possibly heterogeneous adsorbed layers. The fits are shown in the Supporting Information, along with the fitting parameters and plots showing the repeatability of the results. The overall viscoelasticity of the layers is represented by the ratio G''/G' of the layer's loss and storage moduli G_{f} .¹⁷

$$G_{\text{f}} = \mu_{\text{f}} + i2\pi f \eta_{\text{f}} = G'_{\text{f}} + iG''_{\text{f}} \quad (2)$$

where the loss modulus, G'' , is calculated as the product of the sensing frequency (f) and the film's viscosity (η_{f}) which is obtained by modeling the film as the Voigt viscoelastic element (Voigt model) and corresponds to the film's viscosity at the basic resonance frequency of 5 MHz. The storage modulus, G' , is equal to the film's shear elasticity modulus obtained by the fitting to the Voigt model. A high value of G''/G' indicates that the response is dominated by the viscous component, that is, the layer is fluidlike, while a low G''/G' value indicates that the response is more dominated by the elastic component, that is, the adsorbed layer is more solidlike.

The dissipation factor (D) provides a measure of energy losses in the system, and it contains information about film interactions with the bulk solution. Adsorption/desorption as well as structural changes might lead to changes in dissipation. Generally, flat and/or rigid structures have a minimal effect on the dissipation, whereas thick and/or flexible structures increase the dissipation. Hence, dissipation can be seen as a measure of the rigidity or viscoelasticity of the adsorbed film.¹⁴

The instrument used for this study was a Q-Sense E4 device from Q-Sense AB (Göteborg, Sweden) with the capacity to continuously measure the change in frequency and dissipation at the fundamental as well as six overtone frequencies (3rd, 5th, 7th, 9th, 11th, and 13th) in four separate experiment cells, thereby giving the possibility to perform four different experiments at the same time. The large number of overtones was used to gain additional information in terms of viscoelasticity and homogeneity of the adsorbed film through the Voigt model.

The quartz crystal is suspended at the bottom of a temperature controlled measurement cell with a volume of 40 μL . Liquid is sucked through the system first passing through a temperature-controlled loop using a peristaltic pump (Ismatec IPC-N 4).

Experimental Procedure. All but the hydrophobic substrate surfaces were rinsed with Milli-Q and ethanol, gently dried with a stream of nitrogen gas, and then treated in a plasma cleaner (Harrick Scientific Corp., model PDC-32 G, Ossining, NY) in low-pressure air at 30 W for 5 min immediately before use. The hydrophobic substrates were only rinsed with Milli-Q and ethanol and dried with a stream of nitrogen gas. The substrates were then inserted into the QCM instrument, and the fundamental as well as the overtone resonance frequencies were found for each substrate in buffer media. The measuring cells were rinsed several times by pumping buffer media through the system, and the surfaces were then finally left to equilibrate for at least 30 min in order to achieve

(12) Lindh, L.; Svendsen, I. E.; Svensson, O.; Cardenas, M.; Arnebrant, T. *J. Colloid Interface Sci.* **2007**, *310*, 74–82.

(13) Bastardo, L.; Claesson, P.; Brown, W. *Langmuir* **2002**, *18*, 3848–3853.

(14) Rodahl, M.; Höök, F.; Krozer, A.; Brzezinski, P.; Kasemo, B. *Rev. Sci. Instrum.* **1995**, *66*, 3924–3930.

(15) Sauerbrey, G. *Z. Phys.* **1959**, *155*, 206–222.

(16) Höök, F.; Kasemo, B.; Nylander, T.; Fant, C.; Sott, K.; Elwing, H. *Anal. Chem.* **2001**, *73*, 5796–5804.

(17) Voinova, M.; Rodahl, M.; Jonson, M.; Kasemo, B. *Phys. Scr.* **1999**, *59*, 391.

a stable baseline. The experiment was initiated by pumping either BSM (0.20 mg/mL) or LPO (0.10 mg/mL) through the cell for 2 min with a flow-rate of 0.2 mL/min (corresponding to 10 times the cell volume). After exactly 1 h of adsorption, the system was rinsed by pumping pure buffer solution through the cells at a flow rate of 0.2 mL/min for 5 min (corresponding to 25 times the cell volume). The eventual desorption was then allowed to stabilize for 25 min, before adding the second adsorption layer of either BSM (0.20 mg/mL) or LPO (0.10 mg/mL) which was pumped into the measuring cell for 2 min at the flow rate of 0.2 mL/min and then left to adsorb for 1 h, except for the first experiment where LPO was added (to the preadsorbed BSM film) with the initial concentration of 0.010 mg/mL; the concentration was then increased every 30 min to 0.020, 0.030, 0.045, 0.075, and finally 0.10 mg/mL. After the second layer had been adsorbed, the chamber was finally rinsed by once again pumping pure buffer through at a flow rate of 0.2 mL/min for 5 min, and after an equilibration time of 25 min the experiment was stopped. The fundamental resonance frequency as well as all overtones were recorded during the experiments. However, the fundamental frequency is usually not used for analysis, since it often contains interference from standing waves inside the measuring cell and is affected by bulk properties such as flow and bulk viscosity. In the current work, the 3rd, 5th, and 7th overtones were used in the Voigt model (fitting).

Results

The Stepwise Adsorption of LPO onto BSM Preadsorbed Layer. An initial experiment (not shown) was performed in order to identify an appropriate concentration of LPO to adsorb onto the preadsorbed BSM layer. In this particular experiment, the adsorption of BSM (0.2 mg/mL) onto a gold-coated QCM crystal was followed by sequential additions of increasing concentrations of LPO (0.01–0.1 mg/mL). The frequency decreased and the dissipation increased rapidly upon adsorption of the BSM onto the gold surface, and a high sensitivity of the measured signal response to the overtone number was observed, indicating formation of a viscoelastic layer. After rinsing with buffer, the adsorption of LPO onto the BSM layer resulted in a decrease in both frequency and dissipation, indicating an additional adsorbed mass but also an increased viscosity of the protein layers. The magnitude of the change in frequency and dissipation decreased with each new addition of LPO, and at higher concentrations there was very little variation in the signal.

BSM–LPO Adsorption. In all the following experiments, the highest concentration of LPO (0.1 mg/mL) was always used since this concentration gave a large response in both frequency and dissipation. All the following experiments were repeated and showed a good reproducibility; however, for clarity, the plots only show data from one experiment for each system. The reproducibility of the results can be seen in the small deviation in Figure 3, and results are also presented as individual graphs for the raw data of f and D in the Supporting Information. The Voigt model was used in the following experiments to interpret the adsorbed layers in terms of their sensed mass, viscosity and shear elasticity modulus, due to the viscoelastic nature of the adsorbed film.

Figure 1 shows plots of sensed mass (a), viscosity (b), shear elasticity modulus (c), and overall viscoelasticity G''/G' (d) for the sequential adsorption of BSM (0.2 mg/mL) and LPO (0.1 mg/mL) to gold (Au), silica (SiO_2), and hydrophobized silica (hbSiO₂). The adsorption profile of BSM differed greatly depending on the substrate. On gold, the sensed mass showed a Langmuirian adsorption profile with plateau adsorbed amount of 21.5 mg/m² reached after 60 min. On SiO_2 , the adsorption of BSM was very rapid, but significantly lower amounts of BSM

adsorbed onto SiO_2 compared to gold with 5.5 mg/m² adsorbed after 10 min. The calculated sensed mass of BSM adsorbing onto hbSiO₂ showed a markedly different profile compared to hydrophilic SiO_2 or gold. In this case, BSM adsorbed initially rapidly up to about 11.0 mg/m² followed by a slow decrease of the sensed mass down to 7.7 mg/m² after 60 min. Rinsing with a protein-free buffer resulted in a decrease in the sensed mass on SiO_2 and hbSiO₂ by 1.8 and 2.1 mg/m², respectively, while virtually no change in mass was observed for the BSM adsorbed to gold. Despite differences in the sensed mass, the adsorbed mucin had rather similar viscoelastic properties on each substrate, indicating loosely packed layers with relatively low film viscosities and shear moduli. All these layers are highly viscoelastic with G''/G' values larger than 0.5. The addition of LPO solution to the BSM layer resulted in increased sensed mass for the gold and SiO_2 substrates, while the corresponding change in the sensed mass was negligible on hbSiO₂ substrate. The adsorption of LPO resulted in very large changes in the shear elasticity modulus and viscosity for the SiO_2 substrate, while for the gold and hbSiO₂ surfaces the viscosity and shear elasticity changes were significantly lower. After initial abrupt changes in viscosity and shear elasticity modulus, the signals generally remained unchanged on gold and hbSiO₂, while in contrast the viscosity and shear elasticity modulus continued to increase with time on the SiO_2 substrate. The ratio of G''/G' increased on the gold substrate with the addition of LPO, whereas the signal decreased to around 0.6 on hbSiO₂ and for the SiO_2 substrate the ratio of G''/G' decreased to around 0.4 which indicates the formation of a relatively rigid layer.

LPO–BSM Adsorption. Figure 2, shows plots of sensed mass (a), viscosity (b), shear elasticity modulus (c), and overall viscoelasticity G''/G' (d) for the sequential adsorption of the proteins in reverse order, namely, LPO (0.1 mg/mL) followed by BSM (0.2 mg/mL) to gold (Au), silica (SiO_2), and hydrophobized silica (hbSiO₂). Adsorption of LPO is rapid on all substrates. On gold and SiO_2 , the sensed mass showed a Langmuirian adsorption profile with plateau adsorbed amounts of 8.5 and 6.9 mg/m², respectively, reached after 60 min. For LPO adsorption onto a hydrophobic substrate, hbSiO₂, the adsorption profile shows a trend similar to that seen previously for mucin on the same surfaces, namely, a rapid increase in mass followed by a slowly decreasing signal. After rinsing in buffer, the final sensed mass of LPO on hbSiO₂ is significantly lower than that observed on Au and on hydrophilic SiO_2 , with a value of 3.8 mg/m². There is a marked difference in the profiles for the change in viscosity (Figure 2b) and shear elasticity modulus (Figure 2c) for the gold and hbSiO₂ compared to the SiO_2 substrates. For gold and hbSiO₂, the viscosity and elasticity increase rapidly to a large value and then decrease significantly over time, indicating changes in the layer conformation. In contrast, the viscosity changes during LPO adsorption to SiO_2 show a continued increase in signal while the elasticity remains fairly constant over time. The overall viscoelasticity (G''/G') of adsorbed LPO (Figure 2d) is similar for all substrates with a value, after rinsing, of between 0.1 and 0.2. In contrast to the case of mucin (Figure 1d), the LPO layer adsorbs in a much more rigid layer. Addition of BSM to the LPO layer (Figure 2a) results in rapid increased mass for all substrates. A large mass change is associated with BSM onto the LPO-coated gold substrate leading to a total adsorbed mass of around 15 mg/m² after rinsing in buffer. The adsorbed amount of BSM onto LPO-coated SiO_2 leads to a total adsorbed amount of around 8 mg/m². The BSM adsorption onto the LPO-coated hbSiO₂ substrate shows a characteristic sharp peak followed by desorption leading to a final adsorbed mass of around 4.5 mg/m². Adsorption of BSM onto the LPO led

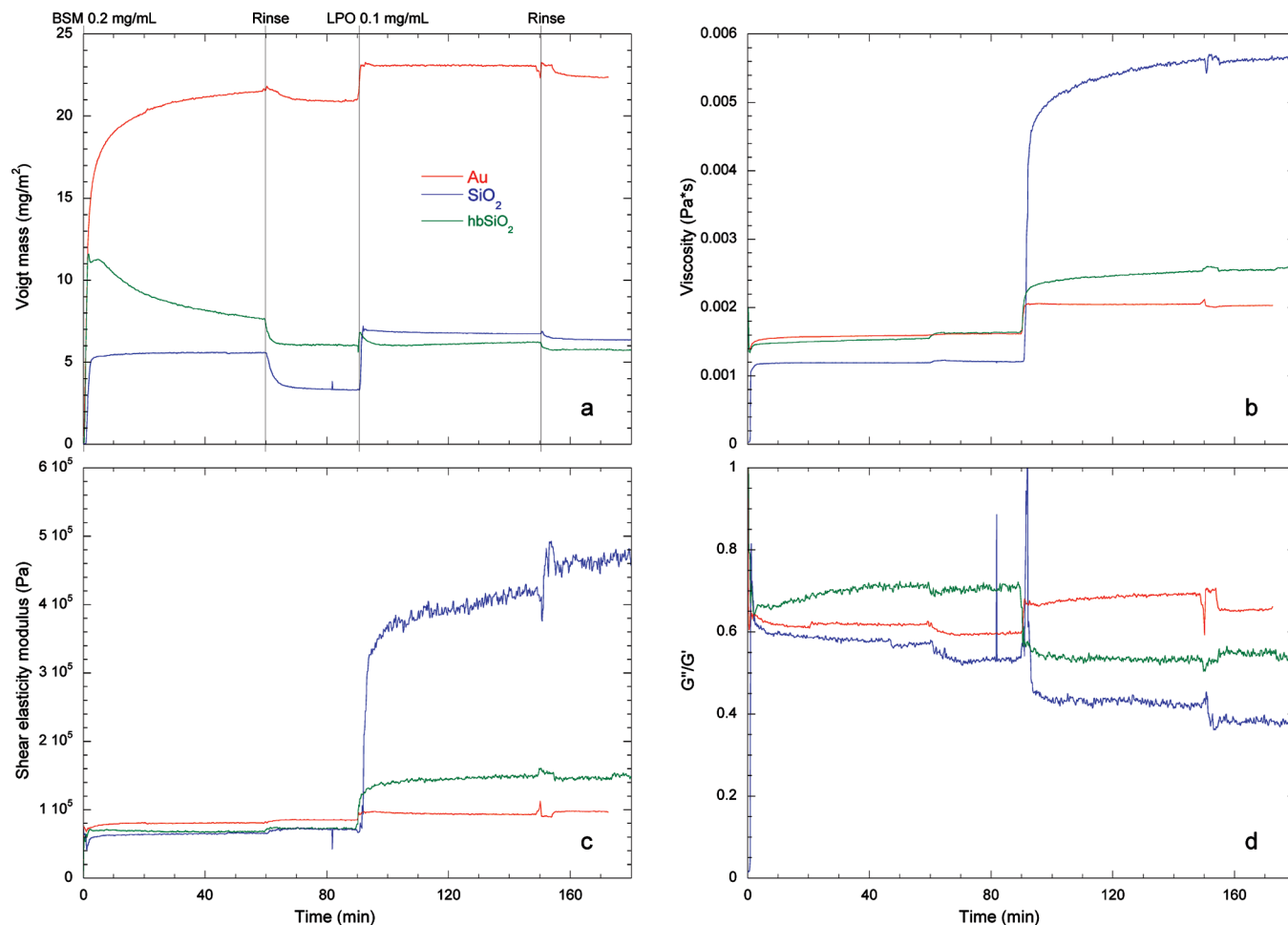


Figure 1. Time evolution of the Voigt mass (a), viscosity (b), shear elasticity modulus (c), and change in G''/G' (d) during adsorption of an initial layer of BSM (0.2 mg/mL) followed by adsorption of LPO (0.1 mg/mL) to gold (red), silica (blue), and hydrophobized silica (green) substrate surfaces.

to a rapid decrease of the shear elasticity and the viscosity of the films adsorbed on gold and SiO_2 (Figure 2b and c). The corresponding changes in viscosity and shear modulus are less pronounced on hbSiO_2 which were already lower than those on gold and SiO_2 . The overall viscoelasticity G''/G' (Figure 2d) increased significantly with BSM adsorption to all substrates to values above 0.5, indicating a diffuse nonrigid layer. However, after rinsing with buffer, a significant reduction in G''/G' is observed for the LPO-coated gold and SiO_2 substrates, leading to a more rigid surface layer most likely due to rinsing away loosely associated molecules. The G''/G' signal is unaffected by rinsing on the LPO-coated hbSiO_2 substrate.

Figure 3 shows the changes in the viscoelastic properties (G''/G') versus the sensed mass for the adsorption of LPO onto BSM-coated substrates (Figure 3a) and for BSM onto LPO-coated substrates (Figure 3b). The G''/G' values for the plot were taken at the plateau of the rinsing parts of the adsorption profiles, when protein solutions were properly exchanged by a rinsing buffer. (More precisely, for each experiment, the G''/G' value is obtained as an average of the G''/G' ratios for the 12 fitted points measured between 25 and 27 min of the rinsing step following the corresponding adsorption step.) The error bars represent the deviation of the fitted values corresponding to two independent experiments performed on separate, newly cleaned substrates in two separate experiments (i.e., not on the same reused substrate). This figure clearly shows that the underlying substrate plays a

significant role in affecting the adsorbed amounts and corresponding viscoelasticity of adsorbed protein films and that the conformational changes of mixed protein layers is highly dependent on the sequence of adsorption. In Figure 3b, The LPO adsorbed to each substrate with a G''/G' value of around 0.2, indicating a rigid adsorbed layer. The adsorbed amount of BSM was lowest for hbSiO_2 and highest for gold. The adsorption of BSM onto LPO-coated substrates resulted in a large increase in G''/G' for all substrates. There was a small mass increase on hbSiO_2 and SiO_2 but a larger increase in adsorbed mass on the LPO-coated gold substrates. The resulting G''/G' was fairly similar after BSM adsorption, yielding values of between 0.5 and 0.6 for the different surfaces. Figure 3a shows that the adsorbed mass of BSM varies significantly depending on the substrate. Relatively little BSM adsorbs to SiO_2 , with an increased adsorption to hbSiO_2 , and a significantly large mass of BSM adsorbs to gold. G''/G' shows variation in the viscoelastic properties of the BSM layer depending on the underlying substrate. BSM adsorbs most rigidly to SiO_2 , whereas the BSM layer is very diffuse on the hbSiO_2 substrate with the gold substrate yielding an intermediate G''/G' . The adsorption of LPO onto the BSM layer results in different mass and G''/G' changes depending on the substrate. For the case of BSM-coated silica, there is a large increase in mass and a large decrease in G''/G' , indicating a more rigid structure in the mixed protein layer. On BSM-coated hbSiO_2 , LPO leads to a significant stiffening of the layer but very

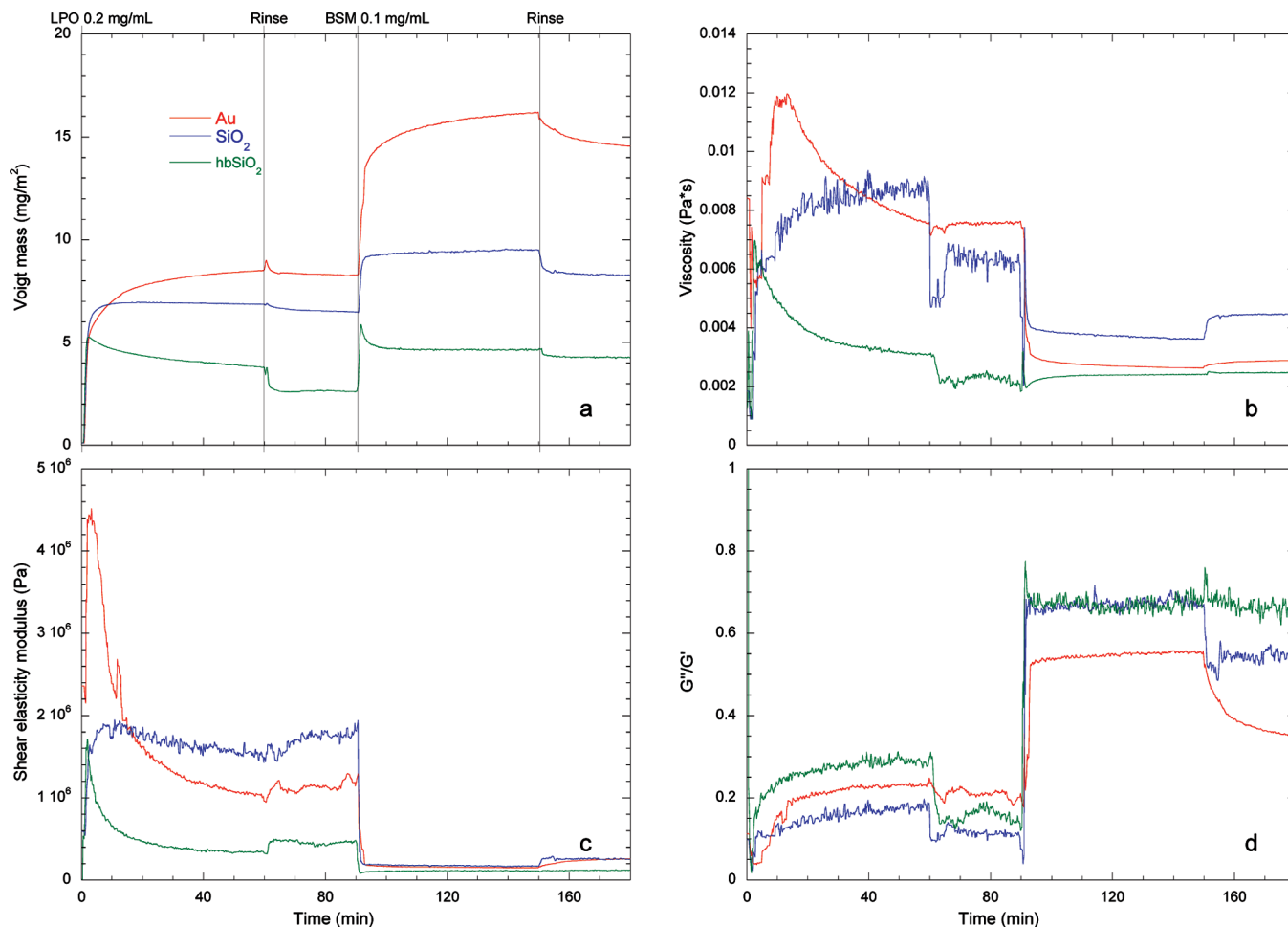


Figure 2. Time evolution of the Voigt mass (a), viscosity (b), shear elasticity modulus (c), and change in G''/G' (d) during adsorption of an initial layer of LPO (0.1 mg/mL) followed by adsorption of BSM (0.2 mg/mL) to gold (red), silica (blue), and hydrophobized silica (green) substrate surfaces.

little mass change. For the case of BSM-coated gold substrates, there is a small mass increase and an increase in G''/G' with the amount of adsorbed LPO.

Discussion

BSM Adsorption on Bare Interfaces. Comparison of the QCM-D results obtained in the current work with results for BSM adsorption obtained by previous ellipsometric studies suggest that highly hydrated mucin films are formed on gold and hydrophilic silica while more dense and less hydrated mucin films adsorb on hydrophobized silica. The adsorption of BSM to gold surfaces has been studied by ellipsometry by Haberska et al.¹⁸ They found that BSM forms a thick film (roughly 35 nm) on gold with an adsorbed amount of about 2 mg/m². Comparing that mass with the calculated sensed mass for BSM on gold in Figure 1 (approximately 21 mg/m²) implies an associated water content of roughly 90%. Svensson et al.¹⁹ investigated adsorption of BSM onto hydrophilic and hydrophobic silica with ellipsometry. The adsorption of BSM to hydrophobic surfaces was found to yield a film thickness of 10 nm with an adsorbed amount of 2 mg/m². In contrast, the adsorption of BSM onto hydrophilic silica was found to be very low with an adsorbed amount of only 0.2 mg/m². The sensed

mass calculated from Figure 1 for BSM adsorbed to hbSiO₂ and SiO₂ suggests a water content of approximately 66% on the hydrophobic silica and approximately 95% water content on hydrophilic silica. Svensson et al. proposed up to 99% water content for BSM adsorbed to silica. In the current study, the adsorbed mass of BSM to gold substrates is up to four times as high as the adsorption to the silica substrates. The adsorbed mucin layer on gold is also more resistant to desorption during rinsing. Compared to silica surfaces, gold has the unique ability to mirror charges which results in strong electrostatic attraction of both positive and negative charges. Moreover, gold is well-known to form strong covalent bonds with thiol groups in adsorbing molecules. The high solvent content of the adsorbed BSM layer indicates that the hydrophilic glycosylated regions extend out to the bulk in long loops and tails. Low values of the layer viscosity and shear modulus are consistent with a layer containing large amount of the trapped solvent. On hydrophilic silica surfaces, the attraction between mucin is expected to be rather weak since both the surface and mucin carry a net negative charge. However, mucin has previously been shown to adsorb to negatively charged surfaces, which is possible since the mucin contains positively charged amino acid residues that can bind to a negatively charged surface as long as the repulsive forces between negative charges are efficiently screened by salt.^{4,20} In this case, the mucin adsorbs

(18) Haberska, K.; Svensson, O.; Shleev, S.; Lindh, L.; Arnebrant, T.; Ruzgas, T. *Talanta* **2008**, *76*, 1159–1164.

(19) Svensson, O.; Lindh, L.; Cardenas, M.; Arnebrant, T. *J. Colloid Interface Sci.* **2006**, *299*, 608–616.

(20) Lindh, L.; Glantz, P.-O.; Carlstedt, I.; Wickström, C.; Arnebrant, T. *Colloids Surf., B* **2002**, *25*, 139–146.

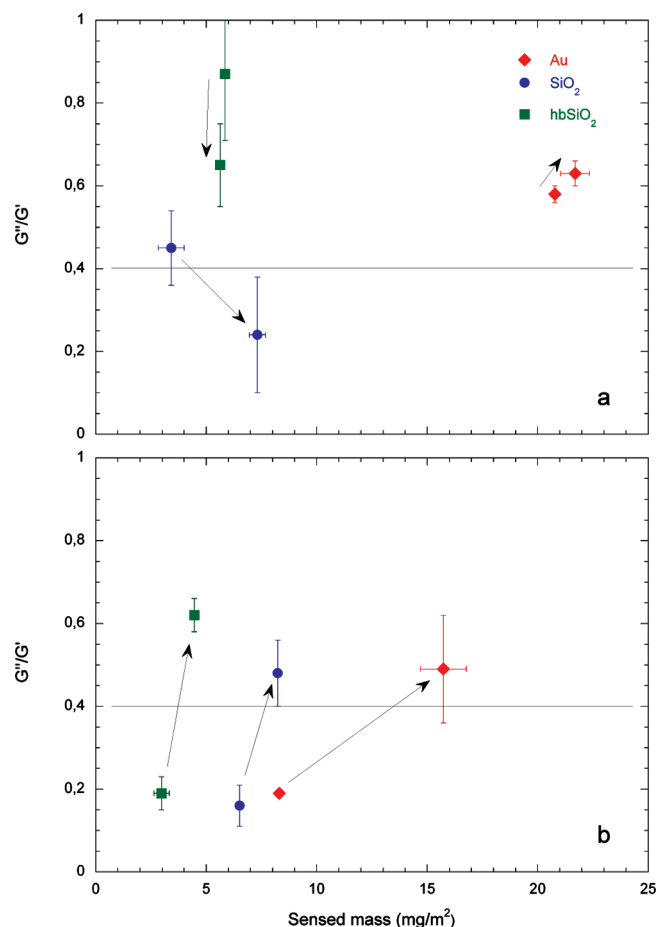


Figure 3. G''/G' value plotted versus Voigt mass for the adsorption of LPO onto BSM-coated substrates (a) and for BSM onto LPO-coated substrates (b). Error bars correspond to the deviation of the values obtained by fitting the data from two independent experiments.

to the surface in an extended conformation closely resembling the conformation in bulk.²¹

The adsorption of mucin to hydrophobized silica is driven by a hydrophobic attraction between the “naked” patches on the mucin backbone and the substrate, leading to an elimination of the entropically unfavorable contact between hydrophobic surfaces and water.^{4,22,23} Since ellipsometry studies calculate similar adsorbed mass of BSM to gold and hydrophobized silica,^{18,19} the lower sensed mass on hydrophobic silica measured by QCM indicates a significantly less hydrated layer, suggesting a different conformation of mucin adsorbed to hydrophobized silica compared to gold. Mucin has been shown to adsorb to hydrophobic surfaces in thin layers, forming thinner layers than mucin adsorbed to charged SiO_2 surfaces, with a more extended structure protruding further into the bulk solution.^{22–24} The decrease observed in the sensed mass following the initial “overshoot peaks”, observed for mucin on hbSiO_2 , may indicate some desorption or conformational changes leading to dehydration of the layer. It is likely that the mucin molecules initially anchor to the surface with a few hydrophobic patches and then change their conformation with increasing number of attachments to the

surface. In this way, the average thickness of the film would gradually decrease along with the solvent content and hence the sensed mass. A small increase in the layer viscosity was observed, which is consistent with the loss of the solvent and an increase of the effective concentration of the mucin molecules in the layer. Interestingly, we did not observe a corresponding increase in the shear elasticity modulus of the layer (which slightly decreased), which is opposite of what we would expect if the only effect would be a relative increase in the effective layer density. The G''/G' value increases slightly during mucin adsorption to hbSiO_2 , indicating that the mucin layer becomes slightly more viscoelastic and less rigid as adsorption proceeds. Mucin contains alternating nonglycosylated parts, which in some cases are globular,²⁵ and glycosylated parts in a random coil conformation. We suggest that the decrease in the layer shear elasticity modulus and the increase in the layer viscoelasticity following the initial mucin adsorption on hbSiO_2 may be caused by a partial unfolding of the globular nonglycosylated parts of mucin molecules during adsorption to the hydrophobic surface. It was previously shown for other globular proteins that the contact with hydrophobic surfaces resulted in unfolding.²⁶ We suggest that molecules adsorbed in the globular state are more elastic (rigid) than the molecules adsorbed in a random coil conformation or denatured globular proteins. It should also be noted that the BSM used in this work was used as received without attempts to purify the mucin. Recent publications^{3,27,28} have shown that the commercial BSM contains small molecular weight protein “contaminants” including a significant quantity of bovine serum albumin (BSA). The small molecular weight proteins have quicker diffusion rates compared to the mucin and result in competitive adsorption to hydrophobic surfaces. The observed “overshoot” in the sensed mass profiles may therefore be rationalized in terms of initial nonspecific adsorption of the small molecular weight fraction of associated proteins followed by displacement by the larger molecular weight mucin. The mass loss is consistent with displacement of the small hydrated proteins and hence removal of extra water. The complementary increase in viscoelasticity is consistent with a more diffuse conformation of the mucin compared to the small molecular weight proteins.

LPO Adsorption on Bare Interface. LPO is a highly surface active protein that readily adsorbs to both hydrophobic and hydrophilic silica surfaces.^{29,30} The adsorption of LPO has been studied previously with ellipsometry^{29,30} and was shown to adsorb faster on hydrophobic surfaces where the asymmetric LPO molecules ($55 \text{ \AA} \times 80 \text{ \AA} \times 80 \text{ \AA}$) (X-ray data from RCSB protein databank 2GJI) adsorb with a side-on orientation, whereas LPO adsorbs somewhat slower to hydrophilic silica surfaces, forming a thicker layer with LPO molecules aligning in a tilted orientation. The current work showed greater adsorption of LPO on SiO_2 compared to hbSiO_2 with a calculated sensed mass of 6.5 and 3.0 mg/m^2 for hydrophilic silica and hydrophobic surfaces, respectively. LPO is positively charged under the conditions used in the present study and so is expected to have attractive electrostatic interactions with the SiO_2 . Ellipsometry measurements

(21) Perez, E.; Proust, J. *J. Colloid Interface Sci.* **1987**, *118*, 182–191.
 (22) Malmsten, M.; Blomberg, E.; Claesson, P.; Carlstedt, I.; Ljusegren, I. *J. Colloid Interface Sci.* **1992**, *151*, 579–90.
 (23) Shi, L.; Caldwell, K. D. *J. Colloid Interface Sci.* **2000**, *224*, 372–381.
 (24) Cardenas, M.; Elofsson, U.; Lindh, L. *Biomacromolecules* **2007**, *8*, 1149–1156.

(25) Yakubov, G. E.; Papagiannopoulos, A.; Rat, E.; Waigh, T. A. *Biomacromolecules* **2007**, *8*, 3791–3799.
 (26) Haynes, C.; Norde, W. *Colloids Surf. B* **1994**, *2*, 517–566.
 (27) Sandberg, T.; Blom, H.; Caldwell, K. D. *J. Biomed. Mater. Res., Part A* **2009**, *91*, 762–772.
 (28) Sandberg, T.; Ott, M. K.; Carlsson, J.; Feiler, A.; Caldwell, K. D. *J. Biomed. Mater. Res., Part A* **2009**, *91*, 773–785.
 (29) Mårtensson, J.; Arwin, H.; Lundström, I.; Ericson, T. *J. Colloid Interface Sci.* **1993**, *155*, 30–6.
 (30) Svendsen, I. E.; Lindh, L.; Arnebrant, T. *Colloids Surf., B* **2006**, *53*, 157–166.

gave adsorbed amounts of 3.7 and 2.7 mg/m² for hydrophilic silica and hydrophobic surfaces, respectively.³⁰ The similarity between the ellipsometric calculated mass and QCM-D sensed mass indicates that the LPO layers on SiO₂ and hbSiO₂ are fairly compact. The associated water included in the sensed mass amounts to 43% on hydrophilic SiO₂ and to 8% on hbSiO₂. The low G''/G' values confirm that the adsorbed LPO layer is rigid.

Recent ellipsometry measurements of LPO adsorption to gold surfaces (Haberska et al.)¹⁸ report an adsorbed mass of 3 mg/m², which is somewhere in between that reported for hydrophilic silica and hydrophobic surfaces). In contrast with the current study, LPO adsorbed with a greater mass on gold compared to the other surfaces. The sensed mass suggests that solvent content in the LPO layer adsorbed on gold is about 64%, which is significantly more than that for layers adsorbed on SiO₂ and hbSiO₂. LPO contains a number of thiol groups which can form covalent sulfide bonds with the gold. However, the thiol containing moieties are not at the surface of the protein, and thus, conformational rearrangements are needed which lead to partial unfolding of the adsorbed LPO molecules. Conformational changes of LPO on gold are strongly supported by the large variation in viscosity and shear elasticity profiles (Figure 2b and c) which show an initial large increase in signal followed by a significant decrease. The fact that very little LPO is removed during rinsing with buffer tends to suggest strong interactions with the surface.

LPO Adsorption to BSM-Coated Surfaces. Complexation and conformational changes of adsorbed BSM layers with smaller charged proteins have been investigated recently with QCM-D. Feiler et al.³ demonstrated the compaction of BSM layers adsorbed to hydrophobic polystyrene by the introduction of BSA. Dedinaite and co-workers^{6,31} and Svensson et al.¹⁹ showed complexation of mucin layers with chitosan. In the case of complexation of mucin with negatively charged BSA, the interaction was attributed to be mainly due to hydrophobic interactions, whereas complexation with chitosan, which carries a net positive charge, could interact via both electrostatic as well as hydrophobic interactions. Similarly, it was assumed that LPO which has a net positive charge under the current solution conditions is likely to interact with BSM via both electrostatic as well as hydrophobic interactions. The effect of introducing LPO to BSM-coated surfaces varied significantly depending on the nature of the underlying surface. With a gold substrate, the addition of LPO resulted in a small increase in sensed mass and a small increase in viscosity and shear elasticity modulus. This indicates incorporation of LPO molecules within the BSM layer. Despite their slight increase, the viscosity and elasticity of the layers on the gold remain relatively low, indicating that the layer remains highly hydrated and viscoelastic which is confirmed with the high G''/G' value. In contrast, the addition of LPO to BSM layers preadsorbed to SiO₂ led to an increase in adsorbed mass and a significantly more rigid layer with a much lower G''/G' value compared to BSM adsorbed by itself. The high values of viscosity and shear elasticity of the final films are similar to those obtained for a LPO layer adsorbed directly on the clean SiO₂ substrate, and therefore, we suggest that LPO molecules adsorb directly on the SiO₂ substrate, which was only scarcely covered by mucin. Attractive electrostatic interactions between the BSM and LPO are possible, since the negatively charged moieties on the BSM will most likely be oriented away from the negatively charged

SiO₂. For BSM layers preadsorbed on hbSiO₂, the addition of LPO led to a significant increase of the layer rigidity despite no detectable change in sensed mass. The interaction of LPO with BSM adsorbed to hbSiO₂ is most likely to occur via electrostatic interactions, since the BSM will be orientated with hydrophobic patches predominately at the surface. The increase in rigidity is assumed to be due to electrostatic complexation of the BSM layer with the positively charged LPO. Displacement of BSM by LPO is unlikely on hbSiO₂ due to the strength of the hydrophobic interaction. It has previously been demonstrated by Brash and Samak³² that exchange of adsorbed blood proteins occurs at a much slower rate at hydrophobic as compared to hydrophilic surfaces.

BSM Adsorption to LPO-Coated Surfaces. In strong contrast to the LPO adsorption to BSM layers, the adsorption kinetics and viscoelastic properties of BSM to LPO-coated surfaces resemble the profiles for BSM adsorption to clean substrates; just the final sensed masses are systematically lower. This suggests that, even in the presence of LPO, BSM adsorbs on the same clean substrates but that the surface availability is reduced due to the presence of adsorbed LPO. The different surface chemistry of the substrates ensures that LPO adsorbs in different conformations which means that the LPO-coated surfaces will also be different for the different substrates. It is therefore unlikely that the LPO-coated surfaces resemble the underlying surfaces to produce the observed BSM adsorption profiles. The resulting viscoelastic properties of the mixed BSM/LPO layers are very similar to the properties of the viscoelastic layers consisting of mucin only, which also indicates that adsorbed mucin molecules have an extended conformation that is similar to that of the mucin adsorbed on the clean substrates. The overall viscoelastic properties of the mixed BSM/LPO layer are dominated by their more viscous part, that is, by the extended, highly hydrated mucin chains.

Conclusion

The adsorbed mass and viscoelastic properties of BSM and LPO layers adsorbing onto gold, silica, and hydrophobized silica have been studied using QCM-D technique. The effect of the order of addition during sequential adsorption of the two proteins has been compared. For BSM, the adsorbed mass, viscosity, shear elasticity modulus, and viscoelastic properties of the adsorbed layer are highly sensitive to the nature of the substrate. BSM adsorbs to gold in a thick highly hydrated viscoelastic layer, while adsorption to silica is lower and leads to a more rigid layer. The adsorption profile of BSM is markedly different on hydrophobized silica compared to gold and silica, since it is dominated by hydrophobic rather than electrostatic interactions. LPO adsorption is different depending on the underlying substrate; however, the adsorbed mass and viscoelastic properties are more similar compared to the variations observed for BSM. The effect of adding LPO to BSM-coated substrates results in different conformational changes and mass uptake depending on the substrate. On BSM-coated gold surfaces, LPO leads to increased mass and viscoelastic properties, while on silica substrates LPO leads to stiffening of the BSM layer due to complexation most probably via hydrophobic interactions. In contrast, BSM adsorbs to LPO-coated surfaces similarly to that on uncoated surfaces which implies that the LPO does not interact significantly with BSM and that LPO adsorption leaves bare patches on the substrate. The study has shown that protein adsorption is highly sensitive to the

(31) Dedinaite, A.; Lundin, M.; Macakova, L.; Auletta, T. *Langmuir* **2005**, *21*, 9502–9509.

(32) Brash, J.; Samak, Q. J. *Colloid Interface Sci.* **1978**, *65*, 495–504.

nature of the substrate and that strategies for designing mixed protein layers for applications should take into account the possible variations in protein conformation and properties in the adsorbed state.

Acknowledgment. We thank the Foundation of Gustav TH Ohlsson for their financial support. We also acknowledge Patrik Bjöörn at Q-Sense AB (Göteborg, Sweden) for valuable

help and for lending us the Q-Sense E4 instrument used in this study.

Supporting Information Available: Theoretical assumptions and details of the fitting procedure as well as graphs with the fitted data and f and D graphs of duplicates for all experiments. This material is available free of charge via the Internet at <http://pubs.acs.org>.